ELSEVIER

Chemical Engineering Journal 77 (2000) 3–9

Chemical Engineering Journal

www.elsevier.com/locate/cej

Tomographic measurements of micro- and macromixing using the dual wavelength photometry

Mathias Buchmann *, Dieter Mewes

Institut für Verfahrenstechnik, Universität Hannover, Callinstrasse 36, D-30167 Hannover, Germany

Abstract

The newly developed tomographical dual wavelength photometry enables the measurement of the local intensity of segregation at a multitude of points inside the stirred vessel. This is done by injecting a mixture of an inert and a reacting dye into the vessel. The inert dye serves as a tracer for the macromixing, whereas the vanishing of the reacting dye shows the micromixing. The concentration fields of the dyes are measured simultaneously by transiluminating the vessel from three directions with superimposed laser beams of different wavelengths. The light absorption by the dyes is measured with CCD-cameras and these projections are used for the tomographic reconstruction of the concentration fields. Low Reynolds number measurements were performed with a combination of two Rushton turbines and a combination of two pitched blade impellers. The combination of the pitched blade impellers yields a good axial transport but a slow micromixing. The injection in the middle between the combination of the two Rushton turbines yields a faster micromixing, but the macrotransport is limited to the region between the stirrers.

Keywords: Micro- and macromixing; Laminar mixing; Optical tomography

1. Introduction

The various aspects of micro- and macromixing have been addressed by a wealth of scientists. The first suggestion for a differentiation between mixing on the macro- and the microscale came from Danckwerts [3]. He introduced the scale of segregation as a measure of the size of the regions of non-homogeneity. The quality of the non-homogeneity between the regions can be described by the intensity of segregation

$$I_S(t) = \frac{\sigma^2(t)}{\sigma_0^2} \quad (1)$$

which is defined as the mean square deviation of the composition from the mean for a given time t compared to the one for $t = 0$.

The direct local determination of these two values is difficult, because this would require measurements on the molecular scale. Käppel [5] and Hiby [4] developed therefore measurement techniques to determine the global intensity of segregation. This is done by adding a discolouration agent to the coloured contents of a mixing vessel. The decreasing colour concentration is measured over time and compared to the initial concentration. This ratio can be used to determine an overall intensity of segregation versus time.

Baldyga and Bourne [2] and Villermaux et al. [12] used a different approach to determine the micromixing time. They inject an agent into the mixing vessel which undergoes a spontaneous reaction. The product R of this reaction reacts with the limiting educt by a fast consecutive reaction to a product S. In the ideal case of instantaneous micromixing only the product R would appear. The final product ratio $2S/(2S + R)$ is therefore linked to the ratio between the time of the consecutive reaction and the micromixing time. This method allows the determination of the micromixing time inside a specific area of the vessel, if the micromixing is fast enough to avoid a spread of the reaction cloud over the whole vessel. In the case of laminar mixing the micromixing is rather slow, so that the spatial resolution of this technique is rough.

Holden et al. [5] use the electrical resistance tomography to measure the distribution of an injected brine solution inside stirred vessels. These measurements are used to evaluate the macromixing.

During the laminar mixing of high viscous non Newtonian liquids phenomena like flow reversal or the formation of cavities occur. The formation of well mixed cavities surrounded by a stagnant liquid was measured and calculated by Nienow et al. [7]. Ottino [8,9] suggested a lamella model to describe the laminar mixing and developed mathematical

* Corresponding author.
E-mail addresses: buch@c36.uni-hannover.de (M. Buchmann), dms@c36.uni-hannover.de (D. Mewes).

1385-8947/00/$ – see front matter
PII: S1385-8947(99)00150-3

methods to describe the stretching and folding of this lamellas by the flow field. His methodology gives insight into the fundamentals of the mixing process itself, but it cannot be used yet to describe the complex process inside stirred vessels.

With the newly developed tomographical dual wavelength photometry, it is possible to measure the local intensity of segregation at a multitude of points simultaneously. With this aim in view a mixture of an inert and a reacting agent is injected into the vessel. The local concentration ratios of the two dyes yield the local intensities of segregation.

2. Experimental technique

2.1. Injection of inert and reacting dye

The course of the laminar mixing process is schematically depicted in Fig. 1. During the first step the length scale of segregation — e.g. the thickness of a lamella — decreases due to the stretching and folding of the injected material. Also, diffusion occurs but its influence is negligible because of the large length scale of segregation. That is why the intensity of segregation remains nearly unchanged, that means that hardly any micromixing occurs. Therefore, a dye that discolours with the vessel contents remains mostly unaffected because the discolouration reaction requires molecular mixing. When the length scale of segregation falls below a certain value, the stronger diffusion levels out local concentration gradients and the intensity of segregation decreases. This second step leads to a reduction of the reacting dye whereas the inert dye remains unchanged from a macroscopic viewpoint. After complete micromixing is achieved only the inert dye remains. The local ratio of the concentration of the reacting dye c_j compared to the concentration of the inert dye c_p describes the intensity of segregation.

In analogy to Danckwerts' [3] intensity of segregation Käppel [6] defined the global degree of deviation Δ as

$$\Delta(t) = \frac{\alpha(t)}{\alpha_0} = \frac{\sum_i |c_{p,i}(t) - \bar{c}_p|}{\sum_i |c_{p,i,0} - \bar{c}_p|} \tag{2}$$

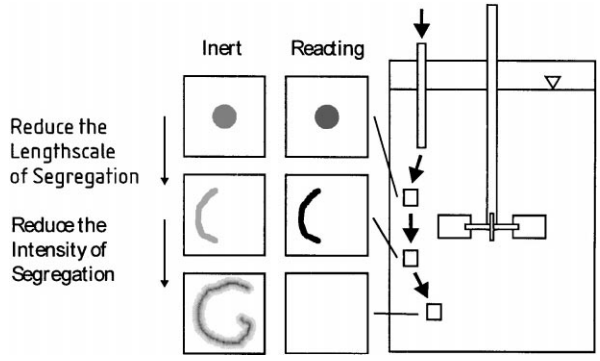

Fig. 1. Course of the laminar mixing process and its influence on inert and reacting dyes.

as the first absolute centered moment of the concentration distribution of an inert dye α at a given time compared to the initial concentration distribution α_0. He also showed that the global degree of deviation is equal to

$$\Delta(t) = \frac{\bar{c}_j(t)}{\bar{c}_{j,0}} \tag{3}$$

that is the ratio of the average concentration of a discolouring dye $\bar{c}_j$ at a given time t compared to its initial average concentration $\bar{c}_{j,0}$, when the dye and the discolouring agent are fed stoichiometrically.

This method only allows global measurements, because the initial concentration according to this definition of an injected droplet at a given location is not known. The local concentration is namely affected by two mechanisms: the first effect is a dilution of the droplet due to the macro transport without micromixing, the second effect is the discoloration after the micromixing. To overcome this problem and separate these two effects, a mixture of an inert dye and a reacting dye is fed into the vessel. The dilution affects both dyes whereas the micromixing only affects the concentration of the reacting dye.

It is now possible to define a local degree of deviation by comparing the local concentration of the reacting dye c_j with the one of the inert dye c_p:

$$\Delta(\vec{x}, t) = \frac{c_j(\vec{x}, t)}{c_p(\vec{x}, t)} K \quad \text{with} \quad K = \frac{c_p(t=0)}{c_j(t=0)} \tag{4}$$

Local concentration means in this case the average concentration in a prismatic element of 3 mm × 3 mm × 3 mm, whose size is determined by the, later described, resolution of the measurement technique. Therefore, the degree of deviation is obtained simultaneously in 36 600 elements throughout the whole mixing vessel. The initial concentration ration K does not effect the measured results. In this case, a ratio K of 0.5 is used because it yields a good contrast between the two dyes.

This local degree of deviation Δ is equal to the 'mixture fraction' defined by Toor [11] and Baldyga [1] as the local ratio of a reacting species compared to a passive tracer. The degree of deviation also shows the same behaviour over time as the intensity of segregation as it decreases from one (totally segregated) to zero (completely mixed). On certain assumptions, it is possible to convert one mixing quality criterion to the other, but to keep the measured results comprehensible only the degree of deviation is used in the figures presented here.

2.2. Experimental setup

The flat-bottomed vessel has a diameter of 100 mm and is filled to a height of 125 mm. Two different stirrer combinations are placed in the centre of the vessel both with a diameter of 50 mm. One combination consists of two six blade Rushton turbines with an axial spacing of 50 mm. The other

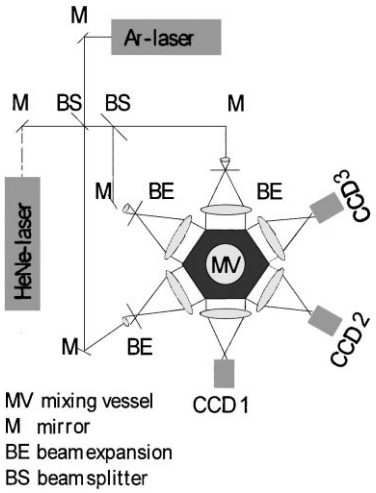

Fig. 2. Optical setup for the tomographical dual wavelength photometry.

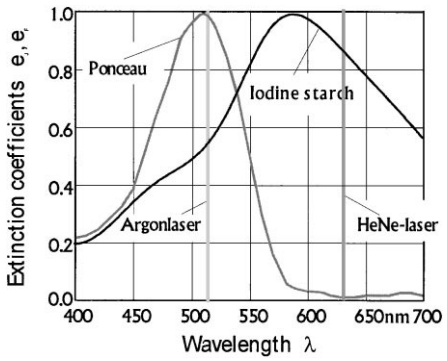

Fig. 3. Extinction coefficients of the dyes and laser wavelengths.

combination consists of two $3 \times 24^{\circ}$-pitched blade impellers with an axial spacing of 50 mm. Both pitched blade impellers are pumping downwards. The stirrer speed of $150\,\mathrm{min}^{-1}$ leads to a Reynolds number equal 10.

2.3. Dual wavelength photometry

The tomographic dual wavelength photometry enables the simultaneous measurement of the two dye concentrations at multiple points in the vessel. The optical set-up is shown in Fig. 2. Two laser beams of wavelength 514 and 632 nm are superimposed in a beamsplitter and then divided into three superimposed beams. The three beams are expanded to a diameter of 150 mm and are used to transilluminate the mixing vessel. The transparent mixing vessel itself is placed inside a hexagonal view bow, which is filled with a refractive index matching liquid. This setup enables the beams to transilluminate the cylindrical vessel without distortion and it also allows a temperature control of the vessel. The beams leave the vessel and give projections of the dye concentrations on RGB-CCD cameras.

The spread of the dye in the vessel is so fast that all projections for the tomographic reconstruction need to be photographed at the same time. This requirement limits the number of projections. Only three cameras are used whose pictures are stored simultaneously in a computer. The cameras deliver pictures at a fixed rate of 25 Hz, but the storage system can be adjusted so that for slower mixing processes the storage frequency is reduced. The projections are used to determine the integrated dye concentrations along the paths of the beams. For that, a reference picture of the vessel without the dye is taken by every camera and is then compared with pictures of the dye projections. The camera signals for a given pixel and the two dye concentrations along the affiliated path are correlated by Lambert–Beer's law

$$A_{514} = (\varepsilon_{\mathrm{P},514} c_{\mathrm{P}} + \varepsilon_{\mathrm{I},514} c_{\mathrm{I}}) b = -\log\left(\frac{I_{514}}{I^0_{514}}\right) \quad (5)$$

$$A_{632} = (\varepsilon_{\mathrm{P},632} c_{\mathrm{P}} + \varepsilon_{\mathrm{I},632} c_{\mathrm{I}}) b = -\log\left(\frac{I_{632}}{I^0_{632}}\right) \quad (6)$$

with I is the light intensity at the pixel for the appropriate wavelength, I^0 the reference light intensity, ε the absorption coefficient, c the concentration along the path and b the length of the path through the vessel.

With the known ε and b and the four measured intensities the two equations yield the two integrated dye concentrations along the path. The wavelength dependence of the absorption coefficient of the reacting dye (iodine starch) and the inert dye (Ponceau) is shown in Fig. 3. The red laser beam is strongly absorbed by the iodine starch but hardly by the Ponceau. On the other hand, the green beam is strongly absorbed by the Ponceau. This inverse wavelength dependence of the absorption coefficients enables precise concentration measurements.

2.4. Tomographic reconstruction

The tomography is used to reconstruct the three dimensional concentration fields from the measured concentrations along the paths. For the reconstruction, the vessel is divided into 30 slices each divided again into 1220 elements yielding a total of 36 600 elements in the whole vessel. The concentration in each of these 36 600 elements is calculated. The arrangement of the elements in a slice is schematically depicted in Fig. 4. Each element belongs exactly to three beams, which improves the quality and the speed of the reconstruction compared to a setup with four beams and quadratic elements. In the later case, beams and elements do not match, so that a weighting function is required that tells which part of the element belongs to which beam.

The reconstruction is done with the iterative algebraic reconstruction technique (ART), as shown by Ostendorf and Mewes [10]. Starting from an assumed concentration distribution in the first slice, the projections for this distribution are calculated. This theoretical set is then compared to the

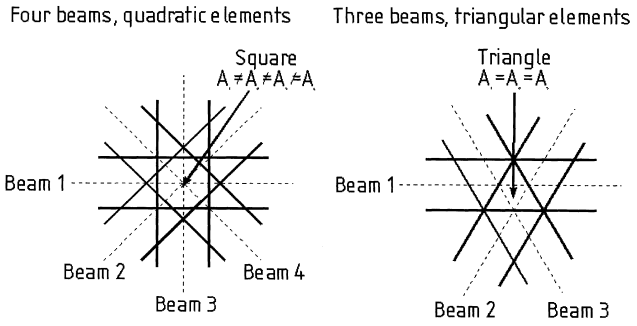

Fig. 4. Tomographic reconstruction with different elements schemes.

actually measured set. The difference between the two sets is fed into an optimiser, where the assumed property distribution is corrected accordingly. This procedure is repeated until a certain error condition is met. Then, the next slice is reconstructed until the field of the whole vessel is determined. In the next step, the whole procedure is repeated for the other dye. Finally, the concentration ratio of reacting and inert dye is calculated for every element to yield the field of the degree of deviation.

The software package AVS is used to visualize the three dimensional fields of the concentration of the inert dye and of the degree of deviation. One feature of the program is the calculation of isosurfaces that connect all points with a specific concentration. The three-dimensional dataset is displayed and can be viewed from different directions. The display of large datasets requires a lot of computational and graphics performance, so that an SGI Onyx Reality Engine[2] is used.

2.5. Material properties

To achieve low Reynolds number mixing the viscosity of the liquid is increased. This is done by dissolving a mixture of 0.1% (w/w) starch, 1% (w/w) carboxymethylcellulose (CRT 10 000 Wolff Walsrode) and 10% sugar (w/w) in the liquid. The sugar is added to match the refractive index of the vessel and the starch is used as iodine indicator. After

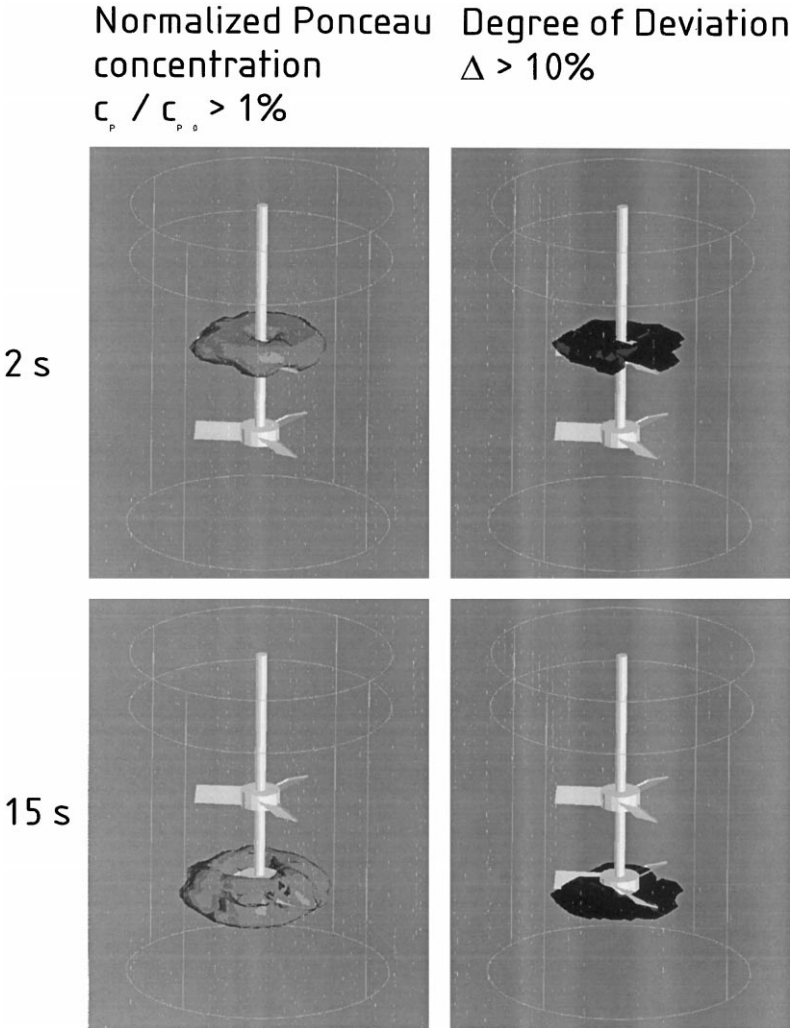

Fig. 5. Mixing with the combination of the two pitched blade impellers.

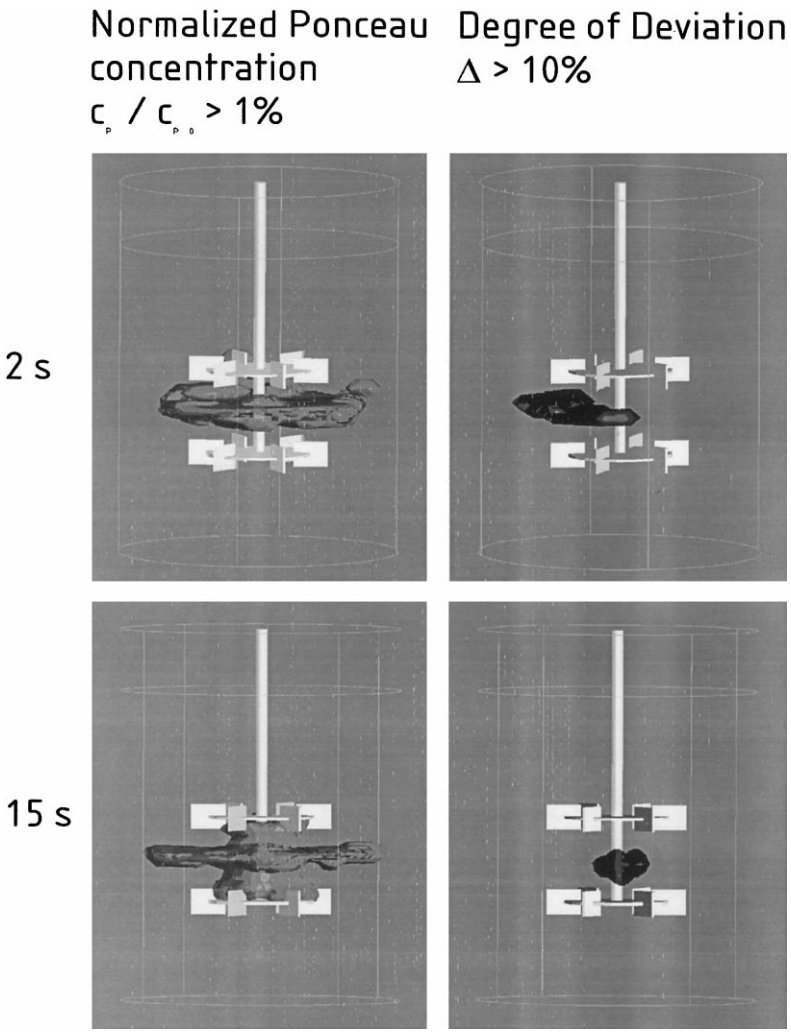

Fig. 6. Mixing with the combination of the two Rushton turbines.

preparing the solution, the part which goes into the vessel is mixed with sodium thiosulfate, whereas the part that is injected is mixed with the two dyes. The reacting dye is the blue iodine starch complex which is discoloured by the reduction of iodine with sodium thiosulfate. The inert dye is red Duasyn Acid Ponceau, which does not react with any of the other chemicals used.

The vessel contains 1 l of liquid and an injected droplet has a volume of 0.25 ml. The molar concentration of iodine in the droplet is twice as high as the sodium thiosulfate concentration in the vessel. These two ratios yield a thiosulfate surplus of 2000 to 1 in the vessel after injection. The huge surplus ensures that the discoloration is not limited by macromixing, as the nearest vicinity of the droplet contains enough thiosulfate to discolour it.

Due to the low concentrations of thiosulfate and of the two dyes, the rheological behaviour of the two liquids is the same. The dissolved cellulose leads to a shear-thinning behaviour of the liquid. Viscosity measurements of the liquid are very well described with the Bird–Carreau model, with a zero shear rate viscosity of 1 Pa s and a power-law index of 0.55.

3. Results and discussion

Figs. 5 and 6 show the course of the macro- and micromixing for the two different stirrer combinations with time. The macromixing is depicted by an isosurface surrounding all volume elements with a local concentration of the inert dye c_p higher than 1% of the initial concentration. Elements outside this dye cloud are basically uncoloured and therefore not macromixed with the injected droplet. The micromixing is depicted by an isosurface surrounding all volume elements with a local degree of deviation Δ higher than 10%. Elements inside this cloud are not sufficiently micromixed yet.

Fig. 5 presents the results for the combination of the two pitched blade impellers. The dye mixture is injected above the upper stirrer. After 2 s, the dye forms one continuous region above the upper stirrer. Therefore, the length scale

of segregation is still high. That results in a slow diffusive transport and a high degree of deviation in most of that region. After 15 s, the dye got transported downwards below the lower stirrer, but it still forms one compact region of approximately the same size it had after 2 s. That means that the dye did not mix effectively with the surrounding liquid, because it still stays in its small region, although that region has moved through the vessel. This ineffective mixing results into a large region that is still not sufficiently micromixed after 15 s.

Fig. 6 presents the results for the combination of the two Rushton turbines. The dye is injected in the middle between the two stirrers. This position in the main suction zone of the stirrers yields a more effective mixing. After 2 s, the droplet is stretched in the radial and circumferential directions, which results in a fast dilution and a fast decrease of the length scale of segregation. The steep gradients enable a strong diffusive transport and, as a result, the degree of deviation is smaller. After 15 s, the dye cloud occupies a larger part of the vessel because the upper part of the dye moves upwards to the upper stirrer, whereas the lower part moves downwards to the lower stirrer. This split of the flow (bifurcation) means a very effective stretching of the injected droplet, which results in a strong decrease of the length scale of segregation. Therefore, most of the injected fluid is micromixed by that time and only a small region has a degree of deviation higher than 10%. This injection position yields better mixing, but no dye is transported above the upper and below the lower stirrer, so that the macromixing is limited to this region of the vessel.

4. Conclusions

The newly developed tomographical dual wavelength photometry gives new insight into the mixing process. With this technique it is possible to measure the local intensity of segregation at multiple points inside the stirred vessel. This is done by injecting a mixture of an inert and a reacting dye into the vessel and by measuring its concentration fields. The inert dye serves as a tracer for the macromixing, whereas the vanishing of the reacting dye describes the micromixing. Measurements were performed with a combination of two Rushton turbines and a combination of two pitched blade impellers. The combination of the pitched blade impellers yields a good axial transport but a slow micromixing. The injection in the middle between the combination of the two Rushton turbines yields a faster micromixing, but the macrotransport is limited to the region between the stirrers.

5. List of symbols

A	absorption, defined in Eqs. (5) and (6)
b	length of the light path through the vessel (m)
$\bar{c}(t)$	average concentration (mol/m^3)
$c(\vec{x}, t)$	local concentration (mol/m^3)
I	light intensity (W/m^2)
I_S	intensity of segregation, defined in Eq. (1)
K	concentration ratio, defined in Eq. (4)
t	time (s)
$\vec{x}$	position vector (m)

Greek letters

α	first absolute centred moment
$\Delta(t)$	global degree of deviation, defined in Eq. (2)
$\Delta(\vec{x}, t)$	local degree of deviation, defined in Eq. (4)
ε	absorption coefficient (m^2/mol)
λ	wavelength (m)
σ^2	mean square deviation

Superscripts

0	reference state

Subscripts

I	iodine
i	summation index
j	reacting dye
P	Ponceau
p	inert dye
0	initial state
514	wavelength = 514 nm
632	wavelength = 632 nm

Acknowledgements

The financial support of the Deutsche Forschungsgemeinschaft is acknowledged.

References

[1] J. Baldyga, Turbulent mixer model with application to homogeneous instantaneous chemical reactions, Chem. Eng. Sci. 44 (1989) 1177–1182.
[2] J.R. Bourne, J. Baldyga, Simplification of micromixing calculations. II. New applications, Chem. Eng. J. 42 (1983) 93–101.
[3] P.V. Danckwerts, The effect of incomplete mixing on homogeneous reactions, Chem. Eng. Sci. 8 (1958) 93–102.
[4] J.W. Hiby, Definition und Messung der Mischgüte in flüssigen Gemischen, Chem. Ing. Tech. 51 (1979) 704–709.
[5] P. Holden, M. Wang, R. Mann, F. Dickin, R.B. Edwards, Imaging stirred vessel macromixing using electrical resistance tomography, AICHE J. 44 (1998) 780–790.
[6] M. Käppel, Entwicklung und Anwendung einer Methode zur Messung des Mischungsverlaufs bei Flüssigkeiten, PhD Thesis, University Munich, Germany, 1976.
[7] A.W. Nienow, T.P. Elson, D.J. Cheesman, X-ray studies of cavern sizes and mixing performance with fluids possessing a yield stress, Chem. Eng. Sci. 41 (1986) 2555–2562.

[8] J.M. Ottino, Mixing and chemical reaction — A tutorial, Chem. Eng. Sci. 94 (1994) 4005–4027.
[9] J.M. Ottino, S.C. Jana, A. Souvaliotis, Potentialities and limitations of mixing simulations, AlChE J. 41 (1995) 1605–1621.
[10] W. Ostendorf, D. Mewes, Measurement of three-dimensional unsteady temperature profiles in mixing vessels by optical tomography, Chem. Eng. Technol. 11 (1988) 148–155.
[11] H.L. Toor, AlChE J. 8 (1962) 70–78.
[12] J. Villermaux, L. Falk, M.C. Fournier, Scale-up on Micromixing Effects in Stirred Tank Reactors by a Parallel Competing Reaction System, 8th European Conference on Mixing, Cambridge, UK, BHRA, 1994, pp. 251–258.